

Supplement of *Clim. Past*, 19, 2535–2550, 2023  
<https://doi.org/10.5194/cp-19-2535-2023-supplement>  
© Author(s) 2023. CC BY 4.0 License.



*Supplement of*

## **Reconstructing atmospheric H<sub>2</sub> over the past century from bi-polar firn air records**

**John D. Patterson et al.**

*Correspondence to:* John D. Patterson ([jdpatter@uci.edu](mailto:jdpatter@uci.edu))

The copyright of individual parts of the supplement might differ from the article licence.

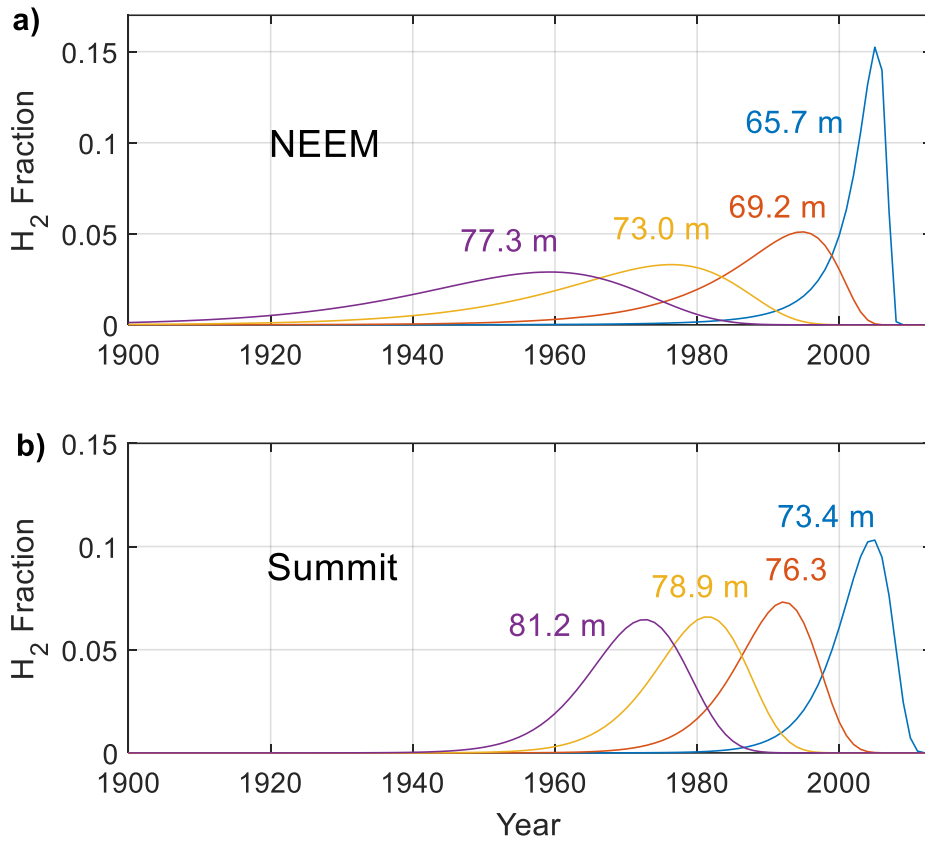
1     **Supplement**

2  
3  
4  
5  
6  
7  
8  
9  
10  
11  
12  
13  
14  
15  
16  
17  
18  
19  
20  
21  
22  
23  
24  
25  
26  
27  
28  
29  
30  
31  
32  
33  
34  
35  
36  
37  
38  
39  
40

14     **Text S1: Calibration of NEEM reconstructions from Petrenko et al., (2013)**

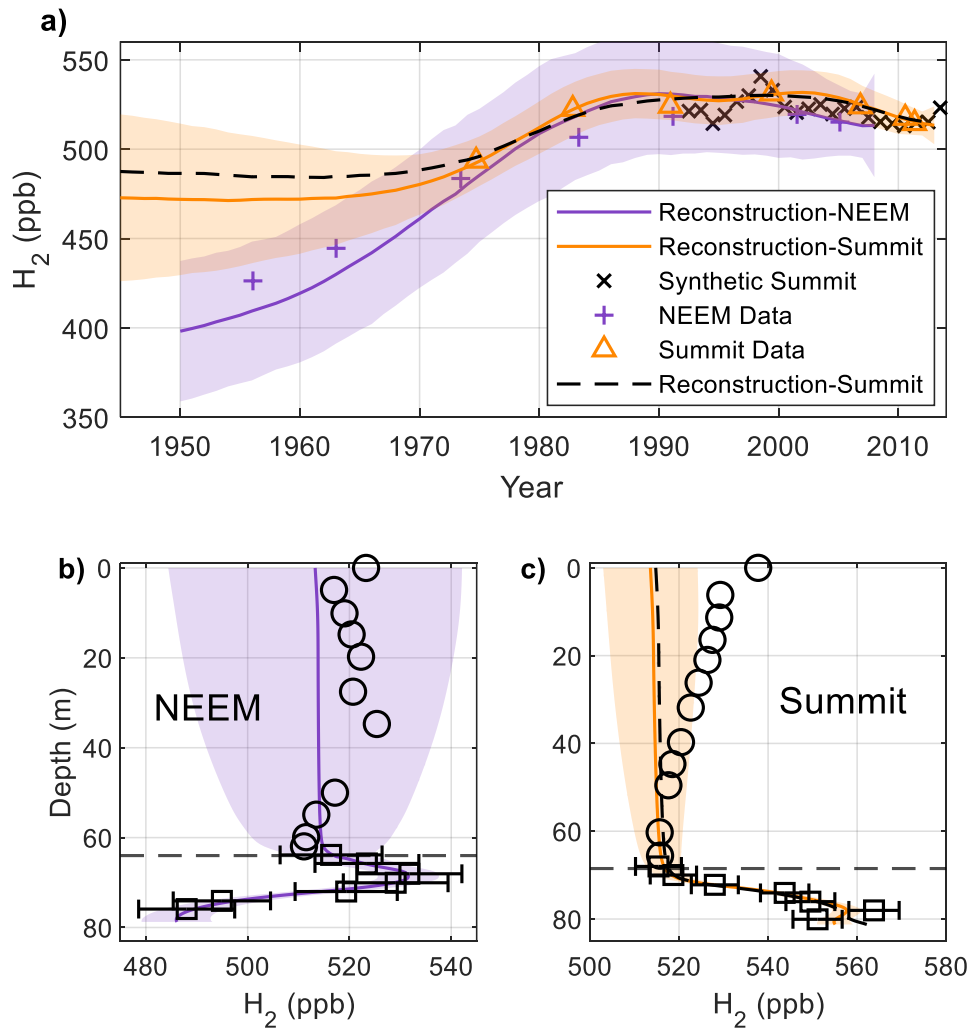
15             The reconstructions published by Petrenko et al. (2013) were based on measurements made at NOAA/GML  
16 on the NOAA96 calibration scale. The NOAA96 calibration scale is known to have drifted over time due to  
17 increasing H<sub>2</sub> in most GML H<sub>2</sub> calibration standards stored in high pressure aluminum cylinders. As a part of the  
18 NEEM firn air sampling campaign (July 2008), matched flask pairs were filled at 12 unique depths. One flask of  
19 each pair was analyzed at NOAA/GML and the other was analyzed at CSIRO. On average, the CSIRO  
20 measurements were 23.8 ppb higher than the NOAA measurements made on the same samples. At that time, CSIRO  
21 was using the CSIRO94 calibration scale. Since then, CSIRO has formally revised their measurements to the MPI09  
22 scale (Jordan & Steinberg, 2011, Section 2.2). On average, the revised measurements are 16.5 ppb higher than the  
23 original measurements. On the basis of these two empirical comparisons, we have added 40.3 ppb (i.e. 23.8 + 16.5  
24 ppb) to the reconstructions published by Petrenko et al. (2013) to correct them to the modern MPI09 calibration. The  
25 corrected reconstructions are plotted in Figure 4a.

41 **Figure S1: Modelled H<sub>2</sub> age distributions (“Green’s functions”) for several depths at NEEM (a) and Summit**  
42 **(b)**



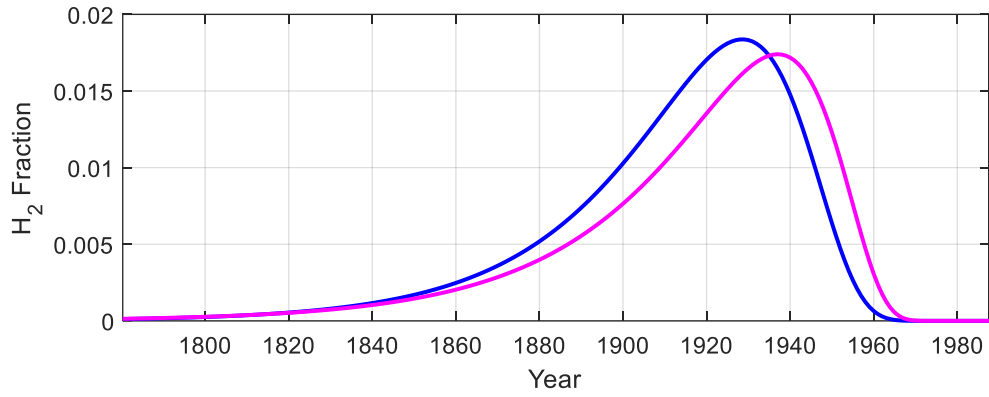
43  
44  
45  
46  
47  
48  
49  
50  
51  
52  
53  
54  
55  
56  
57

58 **Figure S2: Atmospheric histories reconstructed independently from firn air profiles at the two Greenland**  
59 **sites using the *Mitchell\_optimized* configuration. a) purple line and shading- result from NEEM and**  
60 **associated  $\pm 1\sigma$  uncertainty; orange line and shading- result from Summit with the uncertainty on the firn**  
61 **measurements reduced by 50% and associated  $\pm 1\sigma$  uncertainty; dashed black line- the “base-case” Summit**  
62 **reconstruction plotted in Figure 4a; black x’s- annual mean synthetic Summit  $H_2$  history (Section 5; Pétron**  
63 **et al., 2023; Langenfelds et al., 2002), purple crosses and orange triangles- firn data plotted against modeled**  
64 **mean age for NEEM and Summit respectively, the firn data have been adjusted for the effects of pore close-**  
65 **off fractionation; b) black markers- measured  $H_2$  depth profile at NEEM; squares with error bars are**  
66 **measurements used in the reconstruction, and circles are measurements excluded from the reconstruction**  
67 **because of seasonality ; purple line and shading- modeled depth profile using the atmospheric history plotted**  
68 **in purple in a) with the propagated  $\pm 1\sigma$  uncertainty; the dashed black line indicates the top of lock-in zone; c)**  
69 **as in b) for Summit, with the measurement error reduced by 50%; Reducing the uncertainty on the Summit**  
70 **measurements yields  $H_2$  levels 15-20 ppb lower prior to 1975 and very similar levels after 1975. The modeled**  
71 **depth profile in the reduced uncertainty case shows a decreasing trend in the bottom of the firn as is observed**  
72 **in the measurements.**  
73



74  
75  
76

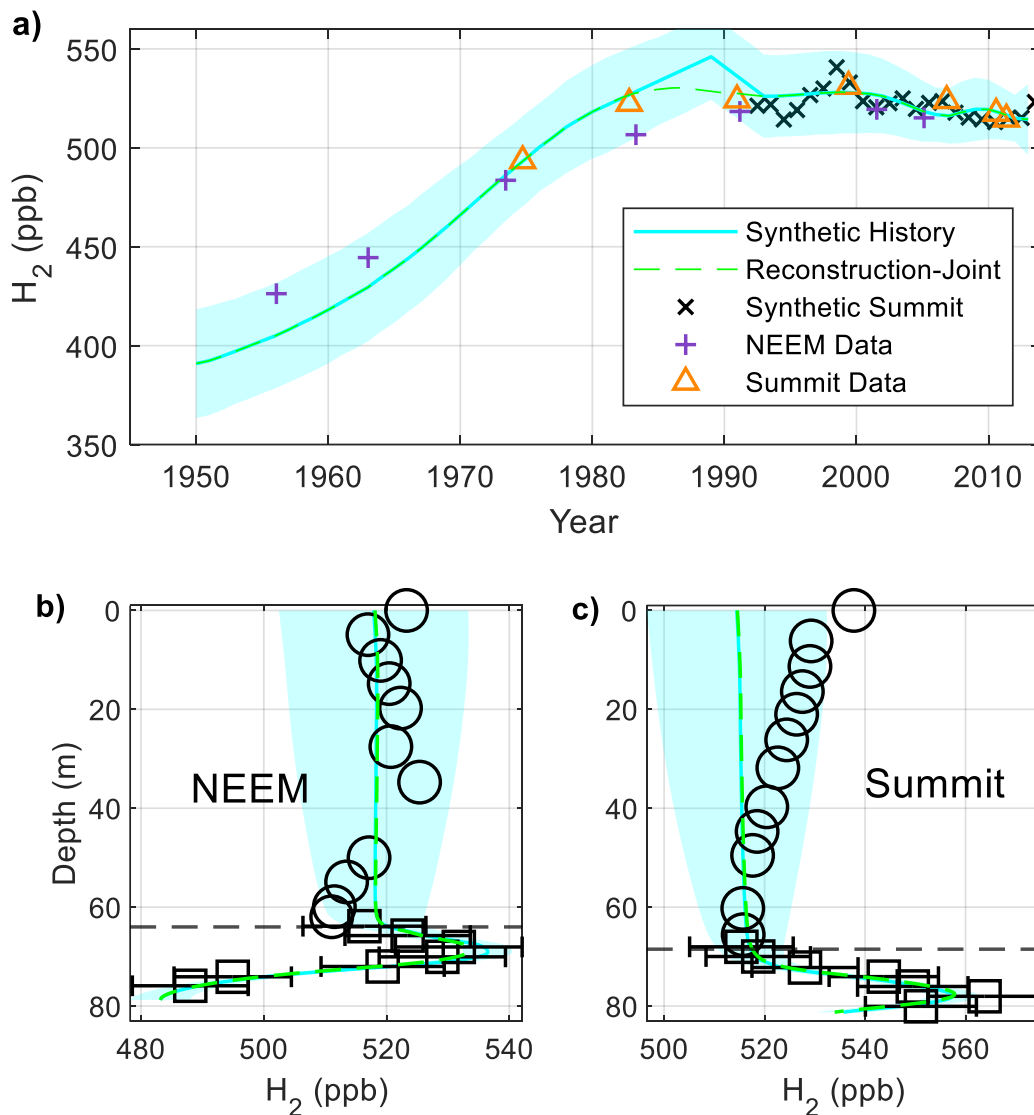
77 **Figure S3: Age distribution (or Green's Function) for H<sub>2</sub> at Megadunes at a depth of 67.4 m calculated with**  
78 **(blue line) and without (magenta line) pore close-off fractionation enabled.**



79  
80  
81  
82  
83  
84  
85  
86  
87  
88  
89  
90  
91  
92  
93  
94  
95  
96  
97  
98  
99  
100  
101

102

103 **Figure S4: The synthetic history used to force the firn air model (blue line and shading in a) and depth**  
104 **profiles generated by the model (blue line and shading in b-c) as described in Section 4. Purple crosses and**  
105 **orange triangles are the firn data plotted against modelled mean age for NEEM and Summit respectively as**  
106 **in Figure 4. Firn air measurements are plotted in b-c as in Figure 4. For comparison, the joint reconstruction**  
107 **and corresponding modeled depth profiles are plotted as dashed green lines. The depth profiles modeled from**  
108 **the synthetic history show good agreement with the measurements.**



109

110

111

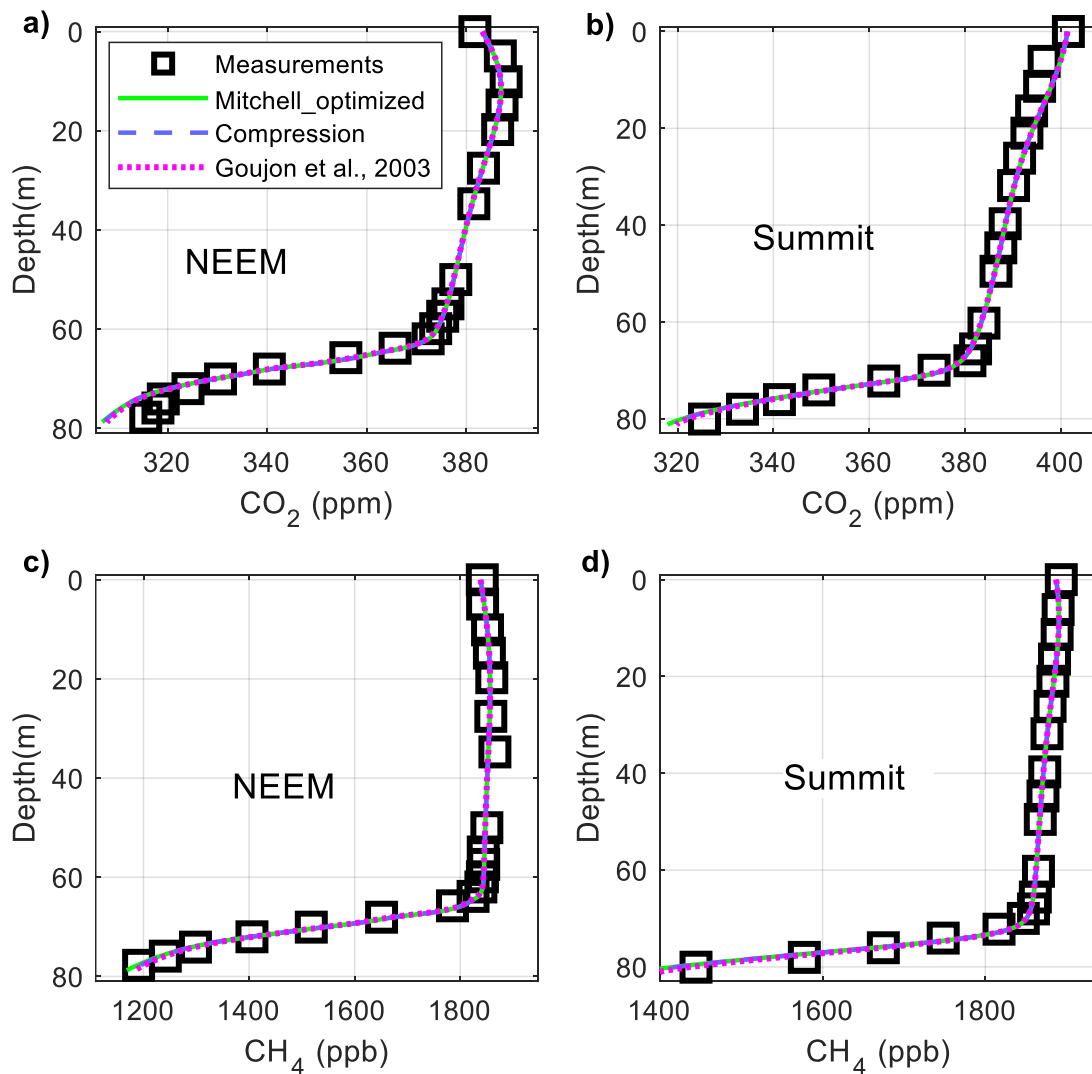
112

113

114

115 **Figure S5: Measured and modeled CO<sub>2</sub> and CH<sub>4</sub> in the firn air at NEEM and Summit using the three model**  
116 **configurations described in Section 3.2: *Mitchell\_optimized* (green lines), *Compression* (dashed purple lines),**  
117 **and *Goujon et al. (2003)* (dotted magenta lines).**

118



119

120

121

122

123

124

125

126

127 **References**

- 128 Goujon, C., Barnola, J. M., & Ritz, C. (2003). Modelling the densification of polar firn including heat diffusion:  
129 Application to close-off characteristics and gas isotopic fractionation for Antarctica and Greenland sites.  
130 *Journal of Geophysical Research D: Atmospheres*, 108(24). <https://doi.org/10.1029/2002jd003319>
- 131 Jordan, A., & Steinberg, B. (2011). Calibration of atmospheric hydrogen measurements. *Atmospheric Measurement*  
132 *Techniques*, 4(3), 509–521. <https://doi.org/10.5194/amt-4-509-2011>
- 133 Langenfelds, R. L., Francey, R. J., Pak, B. C., Steele, L. P., Lloyd, J., Trudinger, C. M., & Allison, C. E. (2002).  
134 Interannual growth rate variations of atmospheric CO<sub>2</sub> and its  $\delta^{13}\text{C}$ , H<sub>2</sub>, CH<sub>4</sub>, and CO between 1992 and  
135 1999 linked to biomass burning. *Global Biogeochemical Cycles*, 16(3).  
136 <https://doi.org/10.1029/2001gb001466>
- 137 Petrenko, V. V., Martinerie, P., Novelli, P., Etheridge, D. M., Levin, I., Wang, Z., Blunier, T., Chappellaz, J.,  
138 Kaiser, J., Lang, P., Steele, L. P., Hammer, S., Mak, J., Langenfelds, R. L., Schwander, J., Severinghaus, J.  
139 P., Witrant, E., Petron, G., Battle, M. O., ... White, J. W. C. (2013). A 60 yr record of atmospheric carbon  
140 monoxide reconstructed from Greenland firn air. *Atmospheric Chemistry and Physics*, 13(15), 7567–7585.  
141 <https://doi.org/10.5194/acp-13-7567-2013>
- 142 Pétron, G., Crotwell, A., Kitzis, M., Madronich, D., Mefford, T., Moglia, E., Mund, J., Neff, D., Thoning, K., &  
143 Wolter, S. (2023). *Atmospheric Hydrogen Dry Air Mole Fractions from the NOAA GML Carbon Cycle*  
144 *Cooperative Global Air Sampling Network, 2009-Present [Data set]*. <https://doi.org/10.15138/WP0W-EZ08>

145

146